Journal of Materials and Environmental Sciences
ISSN : 2028-2508

JMES, 2017 Volume 8, Issue 3, Page 1103-1115

http://www.jmaterenvironsci.com /

Copyright © 2017,
University of Mohammed 1er
Oujda Morocco

First and second order turbulence modeling for flows with recirculation zone: validity of gradient transport hypothesis

R. El Amraoui[*1],H. El Mghari[1], M. Obounou[2], M. Kaddiri[1], M. Mouqallid[3], E. Affad[4], A. Ait Msaad[5], D. Garreton[6]

1 LAMET laboratory, Faculty of Science and Technics, Sultan Moulay Slimane Univ., Béni Mellal, Morocco
2 Dep. of physics, Faculty of Science, Univ. of Yaoundé I, Yaoundé, Cameroun
3Dep. Of energy, Ecole Nationale Supérieure des Arts et Métiers, Univ. Moulay Smail, Meknes, Morocco
4 Dep. of physics, Faculty of Science and Technics, Hassan II Univ., Mohammadia, Morocco
5 High School of Technology, Fes, Morocco
6 EDF-DER-LNH, 6 Quai Watier, Chatou, France

Received 29Aug 2016,
Revised 01Oct 2016,
Accepted 04 Oct 2016

Keywords
- ✓ Second order turbulence modeling
- ✓ k-epsilon model
- ✓ Reynolds stress tensor
- ✓ Gradient transport hypothesis
- ✓ Turbulent Schmidt number.

r_amraoui64@yahoo.fr ;
Phone: +212665669638;
Fax: +212523485201

Abstract

The k-epsilon model is widely used in the simulation of turbulent flows particularly industrial ones. It is based on the gradient transport hypothesis (G.T.H.) proposed by Boussinesq. It introduces the eddy viscosity coefficient calculated from the turbulent kinetic energy k and its dissipation rate ε which are determined by their transport equations. However, the gradient transport assumption is not always valid. So the objective of this work is to further examine the validity of this assumption by simulating a nontrivial flow, like that of bluff body with a recirculation zone behind the obstacle and a stagnation point on the symmetry axis. The full second order model is considered. Thus the Reynolds stresses components and turbulent scalar flux are derived from their transport equations, respectively. The dynamic and scalar fields are examined and the turbulent Schmidt number is analyzed.

1. Introduction :

Reynolds Average Navier Stokes (RANS) is the most used approach to simulate turbulent flows. Indeed, the two other approaches namely DNS (Direct Numerical Simulation) and LES (Large Eddy Simulation) require a number of calculation points often beyond the current computers capacities. Vandromme [1] estimated that number to $R_e^{5/4}$where R_e is the Reynolds number. In the frame of RANS method, momentum and mass conservation equations are averaged with Reynolds or Favre averaging. This procedure leads new unknown terms, which are second order moments or turbulent flux of velocity and scalar.

The basic idea of first order turbulence modeling is the the Boussinesq assumption, i.e. the Gradient Transport Hypothesis (G.T. H.). Hence the Reynolds stress components are connected to the rate of strain with a turbulent viscosity coefficient, whereas with second order turbulence modeling, Reynolds stress and scalar turbulent flux are computed through their transport equations.

Prandtl [2] proposed to link turbulent eddy viscosity ν_t to a characteristic velocity and length scales [3]. Several models were constructed to determineν_t (k-epsilon [4], SST [5] and k-ω [6] ones). The two equations k-epsilon model has been widely used to simulate various turbulent flows, such as two phase flow [7-8], pollutant dispersion [9-11], heat transfer [12] and flow separation [13]. Nevertheless the k-epsilon model predictions are not always good, as it is the case of flows with streamline curvatures or swirl [3]. This is due to the high anisotropy of these flows where the Reynolds stress model gives better results than those obtained with k-ε one. That is why this study is undertaken, to examine the validity of G.T.H. in a complex flow with recirculation and stagnation points. In the same way, it is shown that scalar fields are far from the G.T.H. in the axial direction and also the Schmidt number is not constant, particularly at the two edges of the recirculation zone.

2. Second order turbulence modeling

2.1. Reynolds stress transport equation

The instantaneous equations of mass conservation and momentum [14] are averaged. In the situation of variable density flow, one use Favre averaging because the resulting equations are similar in form to the Reynolds equations for uniform density flow. From these instantaneous equations and after some manipulations, the Reynolds stress equations become as follows:

$$\begin{aligned}
\frac{\partial}{\partial t}\bar{\rho}\widetilde{u_i''u_j''} + \frac{\partial}{\partial x_k}\left[\bar{\rho}\tilde{u}_k\widetilde{u_i''u_j''}\right] = &-\frac{\partial}{\partial x_k}\left[\bar{\rho}\widetilde{u_k''u_i''u_j''} + \delta_{ki}\overline{u_j''p'} + \delta_{kj}\overline{u_i''p'} - \overline{\tau_{ik}u_j''} - \overline{\tau_{jk}u_i''}\right] \longrightarrow \tilde{d}_{ij} \\
&-\bar{\rho}\widetilde{u_i''u_k''}\frac{\partial\tilde{u}_j}{\partial x_k} - \bar{\rho}\widetilde{u_j''u_k''}\frac{\partial\tilde{u}_i}{\partial x_k} \longrightarrow \widetilde{P}_{ij} \\
&-\overline{\tau_{ik}\frac{\partial u_j''}{\partial x_k}} - \overline{\tau_{jk}\frac{\partial u_i''}{\partial x_k}} \longrightarrow \tilde{\epsilon}_{ij} \quad (2.1) \\
&\overline{+p'\left(\frac{\partial u_i''}{\partial x_j} + \frac{\partial u_j''}{\partial x_i}\right)} \longrightarrow \tilde{\phi}_{ij} \\
&-\overline{u_i''}\frac{\partial\bar{p}}{\partial x_j} - \overline{u_j''}\frac{\partial\bar{p}}{\partial x_i} \longrightarrow \widetilde{G}_{ij}
\end{aligned}$$

Where $(\tilde{\ },\ '')$ and $(\bar{\ },\ ')$notations are mean and fluctuation in Favre and Reynolds averaging approaches, respectively.

In their experimental study in an axisymmetric plane channel, Hanjalic and Launder [15] suggested that pressure diffusion term can be neglected. The same authors [16] derived a transport equation for the triple correlation $\overline{u_i'u_j'u_k'}$. Under some assumptions particularly when the convective transport term can be neglected the following algebraic formulae is established:

$$\overline{u_i'u_j'u_k'} = -C_S\frac{k}{\epsilon}\left\{\overline{u_i'u_l'}\frac{\partial\overline{u_j'u_k'}}{\partial x_l} + \overline{u_j'u_l'}\frac{\partial\overline{u_k'u_i'}}{\partial x_l} + \overline{u_k'u_l'}\frac{\partial\overline{u_i'u_j'}}{\partial x_l}\right\} \quad (2.2)$$

Daly and Harlow [17] have proposed the following model for the triple correlation:

$$\overline{u_i'u_j'u_k'} = -C_S\frac{k}{\epsilon}\overline{u_k'u_l'}\frac{\partial\overline{u_i'u_j'}}{\partial x_l} \quad (2.3)$$

Although this expression is much simplest than that of Hanjalic and Launder[16], it remains quite general of Shir's [18] model which is:

$$\overline{u_i'u_j'u_k'} = -C_S\frac{k^2}{\epsilon}\frac{\partial\overline{u_i'u_j'}}{\partial x_k} \quad (2.4)$$

Thus, expression (2.3) uses an anisotropic diffusion coefficient.

The last contribution in the Reynolds stress tensor diffusion $\tilde{d}_{ij}$ is due to viscosity and is assumed to be negligible for high turbulent Reynolds number flows.

The third term on the right hand side of equation (2.1) is the dissipation tensor $\tilde{\epsilon}_{ij}$. It is well known that turbulent energy is dissipated through the smallest eddies, and at high Reynolds number hypothesis these structures are isotropic. Hence, one can write: $\tilde{\epsilon}_{ij} = \frac{2}{3}\delta_{ij}\varepsilon$ where ε is the turbulent kinetic energy dissipation rate and δ_{ij} is the Kronecker symbol.

The fourth term on the right hand side of equation (2.1) is the correlation pressure rate of strain. From the mass and momentum equations, Chou and Quart [19] found the following equation at some point x_0:

$$\overline{\frac{p'}{\rho}\left(\frac{\partial u_i'}{\partial x_j} + \frac{\partial u_j'}{\partial x_i}\right)} = \bar{\phi}_{ij1} + \bar{\phi}_{ij2} + \bar{\phi}_{ijp} \quad (2.5)$$

Where :

$$\bar{\phi}_{ij1} = -\frac{1}{4\pi}\int_{vol}\overline{\frac{\partial^2 u_k' u_l'}{\partial x_k \partial x_1}\left(\frac{\partial u_i'}{\partial x_j} + \frac{\partial u_j'}{\partial x_i}\right)}\frac{d_{vol}}{\mathbf{r}} \; ; \bar{\phi}_{ij2} = -\frac{1}{2\pi}\int_{vol}\frac{\partial \bar{u}_k}{\partial x_l}\overline{\frac{\partial u_l'}{\partial x_k}\left(\frac{\partial u_i'}{\partial x_j} + \frac{\partial u_j'}{\partial x_i}\right)}\frac{d_{vol}}{\mathbf{r}}$$

ϕ_{ij} is the sum of two contributions, each one corresponds to a special physical process. ϕ_{ij1} is the result of mutual interaction between turbulence components, while ϕ_{ij2} arises from interaction between mean rate of strain and fluctuating velocity. The experience shows in the case of grid turbulence decay that flow evolves to an isotropic state. Moreover in this situation only ε_{ij} and ϕ_{ij1} terms are different from zero in equation (2.1). This fact led Rotta [20] to propose the following model:

$\bar{\phi}_{ij1} = -C_1\frac{\bar{k}}{\tau}b_{ij}$, where b_{ij} is anisotropy tensor defined as: $b_{ij} = \frac{\overline{u_i' u_j'}}{\overline{u_i'^2}} - \frac{1}{3}\delta_{ij}$. C_1 is a constant and τ is a characteristic time of the return to the isotropy.τ is assumed to be equal to a turbulent time scale $\tau_t = \frac{k}{\varepsilon}$.

The second part of pressure rate of strain correlation is ϕ_{ij2}. It is qualified as a rapid part and presumed to be responsible of the transmission of any perturbation to the Reynolds stress components. Naot et al. [21] proposed the following expression: $\bar{\phi}_{ij2} = -C_2\left(\bar{P}_{ij} - \frac{2}{3}\delta_{ij}\bar{P}_k\right)$ where $\bar{P}_k = \frac{1}{2}\bar{P}_{ij}$ is the rate of production of turbulent energy, and C_2 is a constant. Launder et al. [22] tried to ameliorate Naot's proposal by using some ideas in the previous work of Rotta [20], they concluded that:

$$\left(\phi_{ij} + \phi_{ji}\right)_2 = -\frac{(C_2 + 8)}{11}\left\{P_{ij} - \frac{2}{3}P\delta_{ij}\right\} - \frac{(30c_2 - 2)}{55}k\left\{\frac{\partial \bar{u}_i}{\partial x_j} + \frac{\partial \bar{u}_j}{\partial x_i}\right\} - \frac{(8C_2 - 2)}{11}\left\{D_{ij} - \frac{2}{3}P\delta_{ij}\right\} \quad (2.6)$$

Where $P_{ij} = -\left\{\overline{u_i' u_k'}\frac{\partial \bar{u}_j}{\partial x_k} + \overline{u_j' u_k'}\frac{\partial \bar{u}_i}{\partial x_k}\right\}$ and $D_{ij} = -\left\{\overline{u_i' u_k'}\frac{\partial \bar{u}_k}{\partial x_j} + \overline{u_j' u_k'}\frac{\partial \bar{u}_k}{\partial x_i}\right\}$

If we contract indices in expression (2.6) each of the three groups of terms on the right side will go to zero. Thus ϕ_{ij2} has a redistributive character. Also Launder et al. [22] show that the first group is a dominant one compared to the two others, and finally ϕ_{ij} can be modeled as Naot's proposal with a change in C_2 constant.

Many other authors (Pope [23], Dibble et al. [24], Janicka [25]) have proposed additional term in the correlation of pressure rate of strain to take into account some effects like low turbulent Reynolds number flows, or relaminarization effect in diffusion flame [26].

The last term on the Reynolds transport equation (2.1) is also unknown. By use of Favre averaging and Reynolds averaging properties, the following relation can be derived [26]: $\overline{u_i''} = \frac{\overline{-\rho' u_i''}}{\bar{\rho}}$ i.e. $\overline{u_i''} = \frac{\nu_t}{\bar{\rho}}\frac{\partial \bar{\rho}}{\partial x_i}$ by means of gradient transport hypothesis.

Taken into account all the previous developments, the Reynolds stress transport equation can be written for high Reynolds number as follows:

$$\frac{\partial}{\partial t}\bar{\rho}\widetilde{u_i'' u_j''} + \frac{\partial}{\partial x_k}\bar{\rho}\tilde{u}_k\widetilde{u_i'' u_j''} = C_s\frac{\partial}{\partial x_m}\left(\bar{\rho}\frac{\tilde{k}}{\tilde{\varepsilon}}\widetilde{u_m'' u_n''}\frac{\partial \widetilde{u_i'' u_j''}}{\partial x_n}\right) - \bar{\rho}\widetilde{u_i'' u_m''}\frac{\partial \tilde{u}_j}{\partial x_m} - \bar{\rho}\widetilde{u_j'' u_m''}\frac{\partial \tilde{u}_i}{\partial x_m}$$
$$-\frac{2}{3}\bar{\rho}\delta_{ij}\tilde{\varepsilon} - C_1\bar{\rho}\frac{\tilde{\varepsilon}}{\tilde{k}}\left(\widetilde{u_i'' u_j''} - \frac{2}{3}\delta_{ij}\tilde{k}\right) - C_2\bar{\rho}\left(\tilde{P}_{ij} - \frac{2}{3}\delta_{ij}\tilde{P}_k\right) - \frac{\nu_t}{\bar{\rho}}\left[\frac{\partial \bar{\rho}}{\partial x_i}\frac{\partial \bar{p}}{\partial x_j} + \frac{\partial \bar{\rho}}{\partial x_j}\frac{\partial \bar{p}}{\partial x_i}\right] \quad (2.7)$$

2.2. Turbulent scalar flux $\widetilde{u_i'' \theta''}$ transport equation

From the transport equations of instantaneous velocity and inert scalar θ, the following equation for $\widetilde{u_i'' \theta''}$ can be derived [26]:

$$\frac{\partial}{\partial t}\bar{\rho}\widetilde{u_i'' \theta''} + \frac{\partial}{\partial x_k}\left[\bar{\rho}\tilde{u}_k\widetilde{u_i'' \theta''}\right] = -\frac{\partial}{\partial x_k}\left[\bar{\rho}\widetilde{u_k'' u_i'' \theta''} + \delta_{ki}\overline{p'\theta''} - \delta_{kj}\overline{\tau_{ij}\theta''} + \delta_{kj}\overline{J_j^{\theta} u_i''}\right] - - - - \rightarrow \tilde{d}_{i\theta}$$

$$-\bar{\rho}\widetilde{u_k''\theta''}\frac{\partial\tilde{u}_i}{\partial x_k}-\bar{\rho}\widetilde{u_i''u_k''}\frac{\partial\tilde{\theta}}{\partial x_k}-\!-\!-\!-\!-\!-\!-\!-\!-\!-\!-\!-\!-\!-\!-\!-\!-\!-\!\rightarrow \tilde{p}_{i\theta}$$

$$-\overline{\tau_{ij}\frac{\partial\theta''}{\partial x_j}}+\overline{J_j^{\theta}\frac{\partial u_i''}{\partial x_j}}-\!\rightarrow \tilde{\varepsilon}_{i\theta} \quad (2.8)$$

$$+\overline{p'\frac{\partial\theta''}{\partial x_i}}-\!\rightarrow \tilde{\phi}_{i\theta}$$

$$-\overline{\theta''}\frac{\partial\bar{p}}{\partial x_i}-\!\rightarrow \tilde{G}_{i\theta}$$

Where J_i^{θ} is the laminar diffusion flux of θ. On the right hand side of equation (2.8) are exposed all the processes contributing to the turbulent scalar flux variation: the diffusion tensor $d_{i\theta}$, the production by mean velocity gradient and mean scalar gradient $P_{i\theta}$, the dissipation tensor $\varepsilon_{i\theta}$, the correlation pressure scalar $\phi_{i\theta}$ and the mean pressure gradient $G_{i\theta}$. In the case of constant density flows all the above processes exist except the $G_{i\theta}$ which is nil. To model Reynolds stress tensor (equation 2.1), the same procedure is used in order to close unknown terms in equation (2.8), especially the pressure scalar correlation $\phi_{i\theta}$ which is modeled through basic idea of Rotta [20] with the return to isotropy (slow part) and isotropisation of production (rapid part). Finally, the following closed scalar flux transport equation for high Reynolds number can be written as:

$$\frac{\partial}{\partial t}\bar{\rho}\,\widetilde{u_i''\theta''}+\frac{\partial}{\partial x_k}\bar{\rho}\tilde{u}_k\widetilde{u_i''\theta''}=C_{s\theta}\frac{\partial}{\partial x_m}\left(\bar{\rho}\frac{\tilde{k}}{\tilde{\varepsilon}}\widetilde{u_m''u_n''}\frac{\partial\widetilde{u_i''\theta''}}{\partial x_n}\right)-\bar{\rho}\widetilde{u_m''\theta''}\frac{\partial\tilde{u}_i}{\partial x_m}-\bar{\rho}\widetilde{u_i''u_m''}\frac{\partial\tilde{\theta}}{\partial x_m}$$

$$-C_{\theta1}\bar{\rho}\frac{\tilde{\varepsilon}}{\tilde{k}}\widetilde{u_i''\theta''}+C_{\theta2}\bar{\rho}\widetilde{u_m''\theta''}\frac{\partial\tilde{u}_i}{\partial x_m} \quad (2.9)$$

2.3. Rate of dissipation of turbulent kinetic energy ε equation

ε is defined as : $\bar{\varepsilon}=\nu\overline{\left(\frac{\partial u_i'}{\partial x_j}\right)^2}$. The transport equation for ε was derived first by Davidov [27] and Harlow and Nakayama [28]. For high Reynolds number it can be expressed as:

$$\frac{D\bar{\varepsilon}}{Dt}=\underbrace{-2\nu\overline{\frac{\partial u_i'}{\partial x_k}\frac{\partial u_i'}{\partial x_l}\frac{\partial u_k'}{\partial x_l}}}_{(i)}\underbrace{-2\overline{\left(\nu\frac{\partial^2 u_i'}{\partial x_k\,\partial x_1}\right)^2}}_{(ii)}\underbrace{-\frac{\partial}{\partial x_k}\left\{\overline{u_k'\varepsilon'}+2\frac{\nu}{\rho}\overline{\frac{\partial u_i'}{\partial x_l}\frac{\partial p'}{\partial x_l}}\right\}}_{(iii)} \quad (2.10)$$

$$\underbrace{-2\left(\overline{\frac{\partial u_i'}{\partial x_l}\frac{\partial u_k'}{\partial x_l}}+\overline{\frac{\partial u_l'}{\partial x_i}\frac{\partial u_l'}{\partial x_k}}\right)\frac{\partial\bar{u}_i}{\partial x_k}}_{(iv)}\underbrace{-2\nu\,\overline{u_k'\frac{\partial u_i'}{\partial x_l}}\frac{\partial^2\bar{u}_i}{\partial x_k\,\partial x_l}}_{(v)}$$

All the terms on the right hand side of equation (2.10) are unknowns and must be modeled. There are: (i): production by vorticity fluctuations, (ii): dissipation of ε by viscosity, (iii): diffusion of dissipation by turbulent flow and pressure fluctuation, (iv): production by mean rate of strain, (v): production by mean dynamic field.
The knowledge of ε leads first to determine the Reynolds stresses through their transport equation and then to have information about length and time scales of turbulent motion. The smallest eddies which are responsible for dissipation of kinetic energy have the following scale: $l_k=C\left(\frac{\nu^3}{\bar{\varepsilon}}\right)^{1/4}$ where ν is the kinematic viscosity and C a constant. Another parameter is the dynamic time scale which can be approximated as: $\tau_t=\frac{\bar{k}}{\bar{\varepsilon}}$. It is of importance in some turbulent combustion models such as the Intermittent Lagrangian Model (MIL model) of Gonzalez and Borghi [29]. In fact the interaction between dynamical scales and chemical ones in these turbulent combustion models leads to the prediction of extinction/re-ignition phenomena in turbulent diffusion flames [30]. The following transport equation for ε is proposed by Hanjalic and Launder [16]:

$$\frac{D\bar{\varepsilon}}{Dt} = C_\varepsilon \frac{\partial}{\partial x_k}\left(\frac{\bar{k}}{\bar{\varepsilon}}\overline{u_k u_l}\frac{\partial \bar{\varepsilon}}{\partial x_l}\right) + C_{\varepsilon 1}\frac{\bar{\varepsilon}}{\bar{k}}\overline{u_i u_k}\frac{\partial \bar{u}_i}{\partial x_k} - C_{\varepsilon 2}\frac{\bar{\varepsilon^2}}{\bar{k}}$$

In his study, MacInnes [31] stated that density variation affects turbulence structures. This effect can be handled by additional of two terms in ε equation. Vandromme [1] proposed to take into account the density variation in the same manner as in turbulent kinetic energy. Thus the source term $\widetilde{G}_\varepsilon$ is as:

$$\widetilde{G}_\varepsilon = -C_{\varepsilon 3}\frac{\tilde{\varepsilon}}{\tilde{k}}\overline{u_i''}\frac{\partial \bar{p}}{\partial x_i} + C_{\varepsilon 4}\frac{\tilde{\varepsilon}}{\tilde{k}}\overline{p'\frac{\partial u_i''}{\partial x_i}}$$

Finally the following transport equation for ε is retained [26]:

$$\frac{\partial}{\partial t}\bar{\rho}\tilde{\varepsilon} + \frac{\partial}{\partial x_k}\bar{\rho}\widetilde{u_k}\tilde{\varepsilon} = C_\varepsilon \frac{\partial}{\partial x_m}\left(\bar{\rho}\frac{\tilde{k}}{\tilde{\varepsilon}}\overline{u_m'' u_n''}\frac{\partial \tilde{\varepsilon}}{\partial x_n}\right) - C_{\varepsilon 1}\bar{\rho}\frac{\tilde{\varepsilon}}{\tilde{k}}\left(\overline{u_i'' u_m''}\frac{\partial \tilde{u}_i}{\partial x_m} + \frac{\nu_t}{\bar{\rho}^2}\frac{\partial \bar{\rho}}{\partial x_i}\frac{\partial \bar{p}}{\partial x_i}\right) - C_{\varepsilon 2}\bar{\rho}\frac{\tilde{\varepsilon}^2}{\tilde{k}} \quad (2.11)$$

In this study the second order turbulence model is a set of equations: (2.7) for Reynolds stresses, equation (2.9) for turbulent scalar flux and equation (2.11) for the kinetic energy dissipation rate ε. The values of all constants are specified in table 1, just below:

Table 1: Constants of second order turbulence model

C_1	C_2	$C_{\theta 1}$	$C_{\theta 2}$	C_s	C_ε	$C_{s\theta}$
1.8	0.6	3	0.5	0.22	0.18	0.18

3. First order turbulence modeling: k-ε model

Reynolds stress tensor is not computed by its transport equation like in the previous section but from an algebraic relation. Boussinesq in 1877 proposed a similar relationship to that of the viscous tensor in case of Newtonian fluid. Thus the shear stress is as : $-\overline{u'v'} = \nu_t\frac{\partial \bar{u}}{\partial y}$ (2.12). Where ν_t is the turbulent eddy viscosity. It depends not on the fluid properties but on the flow characteristics. The equation (2.12) can be generalized as:

$$-\overline{u_i'u_j'} = \nu_t\left(\frac{\partial \bar{u}_i}{\partial x_j} + \frac{\partial \bar{u}_j}{\partial x_i}\right) - \frac{2}{3}\delta_{ij}\bar{k} \quad (2.13)$$

The equivalent of equation (2.13) for an inert scalar θ is: $\overline{u_i'\theta'} = \frac{\nu_t}{Sc_\theta}\frac{\partial \bar{\theta}}{\partial X_i}$ (2.14). Where Sc_θ is a turbulent Schmidt number. Equations (2.13) and (2.14) are called a gradient transport hypothesis.

The gradient transport laws are very simple in implementation. However, their failure has been established in many cases. Thus, the experimental investigation of a parietal jet by Tailland and Mathieu [32] shows that $\frac{\partial \bar{u}}{\partial y}$ does not vanish in the same place as $\overline{u'v'}$. Also counter gradient situations have been shown in the literature. That is the case of Starner and Bilger's [33] study in a turbulent diffusion flame.

The proportionality coefficient between Reynolds stress and rate of strain is the turbulent eddy viscosity ν_t. Prandtl [2] has linked ν_t to a characteristic velocity V and a characteristic length scales l of the flow; thus: $\nu_t = V * l$. V and l are determined empirically. This model is known as zero equation model. Thereafter, the calculation of the velocity characteristic has been improved. Indeed, V is connected to the square root of the turbulent kinetic energy k, which is given by its transport equation. Thus: $\nu_t = \sqrt{\bar{k}}l$. This is the model of Prandtl-Kolmogorov known as the one equation model. This model remains dependent on the length scale whose determination is difficult in the case of complex flows. Kolmogovov [34] proposed to link the length scale to the two main variables of the turbulent flow k and ε according to the relationship: $l = \frac{\bar{k}^{3/2}}{\bar{\varepsilon}}$ which with the above equation for l gives: $\nu_t = \frac{\bar{k}^2}{\bar{\varepsilon}}$ (2.15). This is the two-equation model known as the k-ε model.

It should be noted that in the context of the second order turbulence models, the resolution of the k equation is not necessary. Physically k represents the energy of turbulent motion, which is contained in large structures. The k equation is obtained from the Reynolds stresses by contraction of the indices i and j in equation (2.1) ($\tilde{k} = \frac{1}{2}\widetilde{u_i'' u_i''}$). Thus:

$$\begin{aligned}
\frac{\partial}{\partial t}\bar{\rho}\tilde{k} + \frac{\partial}{\partial x_k}\left(\bar{\rho}\tilde{u}_k\tilde{k}\right) = &-\frac{\partial}{\partial x_k}\left[\bar{\rho}\widetilde{u_k'' u_i'' u_i''} + \delta_{ki}\overline{u_i' p'} - \overline{\tau_{ik} u_i''}\right] \longrightarrow \tilde{d}_k \\
&-\bar{\rho}\widetilde{u_i'' u_k''}\frac{\partial \tilde{u}_i}{\partial x_k} \longrightarrow \tilde{P}_k \\
&-\overline{\tau_{ik}\frac{\partial u_i''}{\partial x_k}} \longrightarrow \tilde{\epsilon} \quad (2.16) \\
&+\overline{p'\frac{\partial u_i''}{\partial x_i}} \longrightarrow \tilde{\phi}_k \\
&-\overline{u_i''}\frac{\partial \bar{p}}{\partial x_i} \longrightarrow \tilde{G}_k
\end{aligned}$$

The five terms on the right hand side of equation (2.16) have the same meaning as in equation (2.1).
Related to isovolume case, the k equation reveals two additional contributions: the correlation pressure divergence ϕ_k and the mean pressure gradient term G_k. According to Bilger [35], these two contributions can represent the turbulence generated by the flame. The closure procedure of ϕ_k term is based on the basic ideas of Rotta [20] and Naot et al. [21]. The other terms are modeled in a similar manner that the Reynolds stresses using the gradient transport hypothesis for turbulent flux of velocity and scalar.

Finally in the frame of first order turbulence modeling the k and ε equations can be written as follows:

$$\frac{\partial}{\partial t}\bar{\rho}\tilde{k} + \frac{\partial}{\partial x_i}\bar{\rho}\tilde{u}_i\tilde{k} = \frac{\partial}{\partial x_i}\left[\left(\mu + \frac{\mu_t}{\sigma_k}\right)\frac{\partial \tilde{k}}{\partial x_i}\right] + \bar{\rho}\widetilde{P_k} - \bar{\rho}\tilde{\varepsilon} - \frac{\nu_t}{\bar{\rho}}\frac{\partial \bar{\rho}}{\partial x_i}\frac{\partial \bar{p}}{\partial x_i} \quad (2.17)$$

$$\frac{\partial}{\partial t}\bar{\rho}\tilde{\varepsilon} + \frac{\partial}{\partial x_i}\bar{\rho}\tilde{u}_i\tilde{\varepsilon} = \frac{\partial}{\partial x_i}\left[\left(\mu + \frac{\mu_t}{\sigma_\varepsilon}\right)\frac{\partial \tilde{\varepsilon}}{\partial x_i}\right] + C_{\varepsilon 1}\bar{\rho}\frac{\tilde{\varepsilon}}{\tilde{k}}\left(\widetilde{P_k} - \frac{\nu_t}{\bar{\rho}^2}\frac{\partial \bar{\rho}}{\partial x_i}\frac{\partial \bar{p}}{\partial x_i}\right) - C_{\varepsilon 2}\bar{\rho}\frac{\tilde{\varepsilon}^2}{\tilde{k}} \quad (2.18)$$

Where :

$$\widetilde{P_k} = -\mu_t\frac{\partial \tilde{u}_i}{\partial x_j}\left(\frac{\partial \tilde{u}_i}{\partial x_j} + \frac{\partial \tilde{u}_j}{\partial x_i}\right) - \frac{2}{3}\tilde{k}\frac{\partial \tilde{u}_k}{\partial x_k} - \frac{2}{3}\mu_t\left(\frac{\partial \tilde{u}_k}{\partial x_k}\right)^2$$

is the production of turbulent kinetic energy.

The constants of the k-ε model are given in the table 2 just below:

Table 2: Constants values of k-ε turbulence model

C_μ	$C_{\varepsilon 1}$	$C_{\varepsilon 2}$	σ_k	σ_ε
0.09	1.44	1.92	1	1.3

4. Application

4.1.Numerical method

Computations were performed with a two dimensional ESTET numerical code, which was developed in LNH-EDF Laboratory (Chatou, France). It is based on finite difference approach. Instead of solving the differential equation relevant of the total balance one, it solves simple differential equations type convection or diffusion. Convection is solved with a two dimensional characteristics method, using third order space interpolation, diffusion and source term step is solved with a semi-direct implicit method after splitting into orthogonal directions. Pressure is located at the center of meshes and determined with a Poisson equation, which is treated

with a conjugate gradient method. To avoid numerical oscillations, the Reynolds stress and scalar turbulent flux components are computed on the pressure half staggered subgrid. Special efforts have been made to minimize the CPU time increase and to get a numerically stable coupling between Navier Stokes and Reynolds stress equations. Conventional wall functions (linear or logarithmic laws) are used for solid wall conditions.

4.2. Test case description

The flow configuration consists of a 5.4 mm diameter jet of methane (21m/s) located at the center of a cylindrical bluff body. The air is supplied through a coaxial jet surrounding the bluff body between diameters of 50 mm and 100 mm. The experiment has been conducted in an unconfined case and corresponds to a blockage ratio of 25% (figure 1).

Fine measurements were performed in the inert and reactive cases by Sandia national laboratories and Gaz de France [36]. The experiment shows at high air velocity (25m/s) that the methane jet is entirely blocked by air flow and two stagnation points are observed on the center line, respectively at 40 mm and 65 mm from the jet exit (Figure 2 : the N case). The solid lines represent zero iso mean axial velocity. The recirculation zone is located between the two lines, with two counter-rotating eddies. When air velocity decrease, the first stagnation point goes downstream toward the second. The two points coincide for a mean air velocity equal of 15 m/s (Figure 2: the M case). And for low air velocity the methane jet penetrates completely with a displacement of the stagnation point from the symmetry axis (Figure 2: the L case whose mean air velocity is equal to 7.5 m/s).

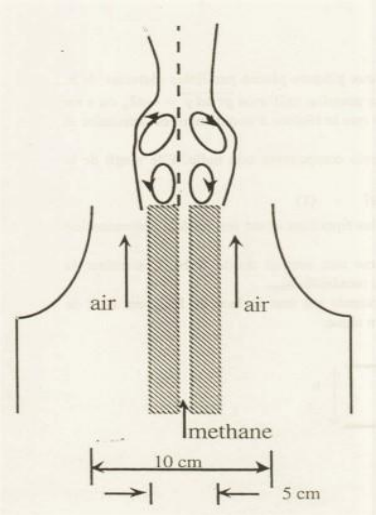

Figure 1 : Experimental setup

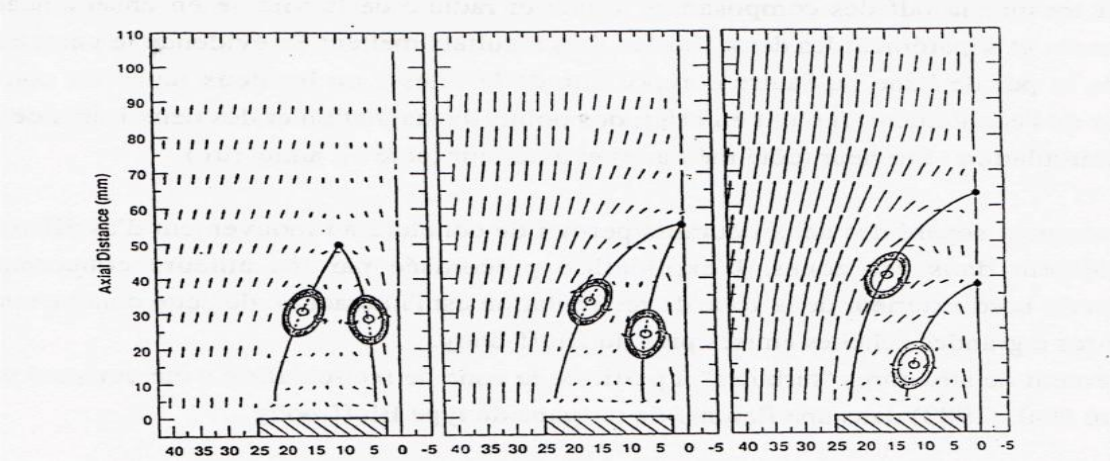

Case L Case M Case N

Figure 2 : Zero iso mean axial velocity lines from Schefer et al' experience[36]

5. Results and discussions

The sensitivity of the results to the inlet conditions of both jets has been tested and found to be important. As expected, the mean velocity profile and the turbulence level of the methane inlet jet have a great influence on the first stagnation point location (on the axis), while the second stagnation point is much more determined by the same parameters of the air inlet. The length of the upstream methane pipe is long enough to allow fully developed turbulence pipe conditions for the central jet. Moreover the air flow inside the burner has been computed to provide realistic conditions at the axis. The computations are performed with a grid of 72x125 nodes, representing respectively 175 mm radially and 270 mm axially. The grid independence has been checked with a grid of 116x214. For more details about the computational domain see the reference [37].

In this study we are interested in the simulation of the bluff body inert case M which corresponds to the central methane mean velocity jet equal to 25m/s surrounded by an air coflow with 15m/s for bulk velocity. The computations are made with two turbulence models. The first one is the k-ε model whose equations are developed in section 3, the second model is the Reynolds stress model (RS model) with full second order modeling, i.e. transport equations for Reynolds stress tensor and turbulent scalar flux are resolved. Velocity vector field computed with the RS model is depicted on Figure 3. Thus the flow presents a large recirculation zone downstream the bluff body which does not enter the central jet. Along the axis, the velocity exhibits a minimum positive value in accordance with the experimental observations of Schefer et al. [36].

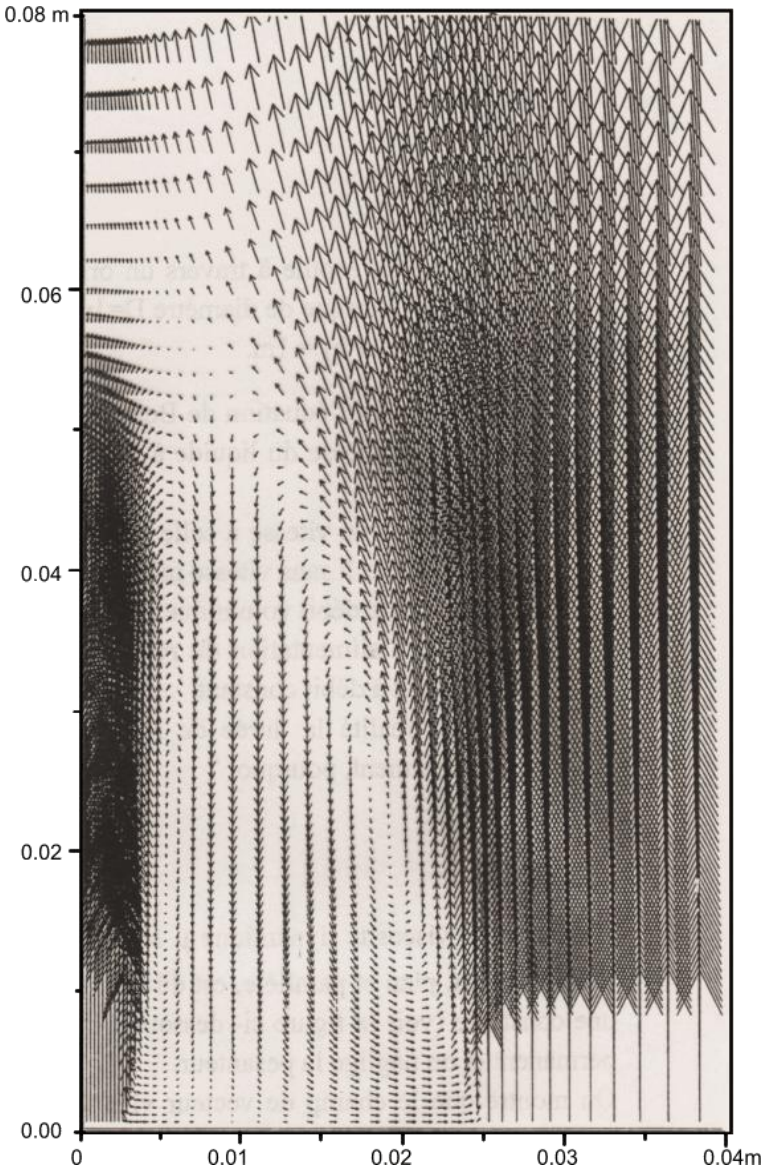

Figure 3 : Velocity vector field computed with RS Model

For more detailed analysis, the mean axial velocity computed with k-ε model and RS model compared to measurements is depicted on Figure 4.We distinguish four characteristic zones of the axial development of the flow: i) first, the potential region, wherein the mixture has not yet performed and where the average values of velocity and scalar are constant ; ii) decreasing zone, which characterizes the central jet penetration ; iii) minimum velocity zone, called stagnation region where the axial mean velocity is close to zero. Methane there are trace; iv) the reattachment zone: the flow of air joins the axis of symmetry, it is accelerating and moving towards a free jet type flow.

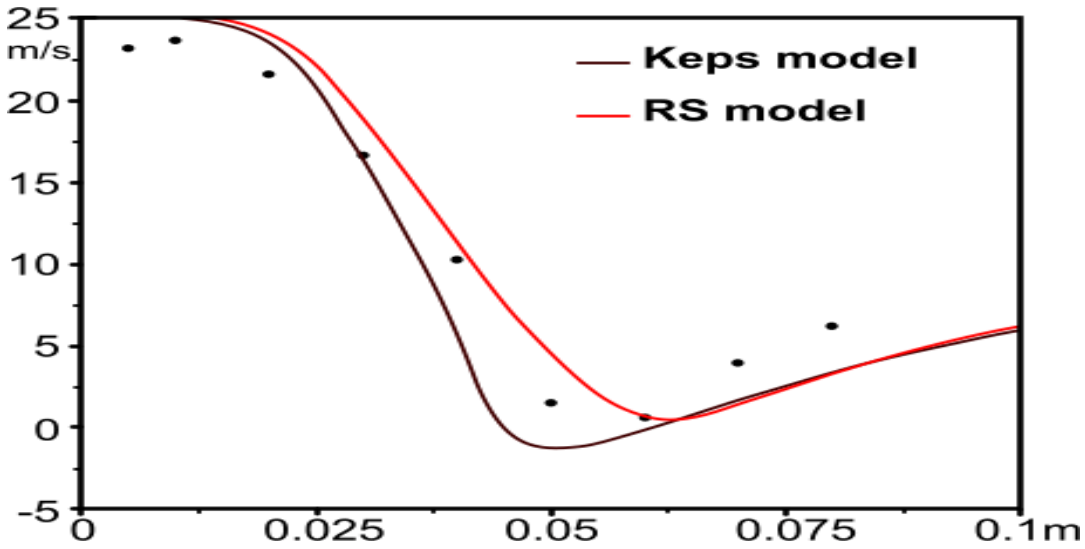

Figure 4 : Axial evolution of mean axial velocity on the symmetry axis

As regards the axial mean velocity, the k-ε model predicts a higher decrease rate, therefore a low penetration of the jet. In addition, at the stagnation region, there is the existence of two points of zero velocity with a negative mean axial velocity zone extending over 15 mm. The predictions of RS model are better than those of the model k-ε, however the position of the minimum axial velocity point is moved slightly downstream.

Concerning the inert scalar results, experience indicates a change of the decay slope at 40 mm from the burner nozzle. The k-ε model seems to capture this phenomenon, however it greatly underestimates the penetration of the jet, while the predictions of RS model are better (Figure 5).

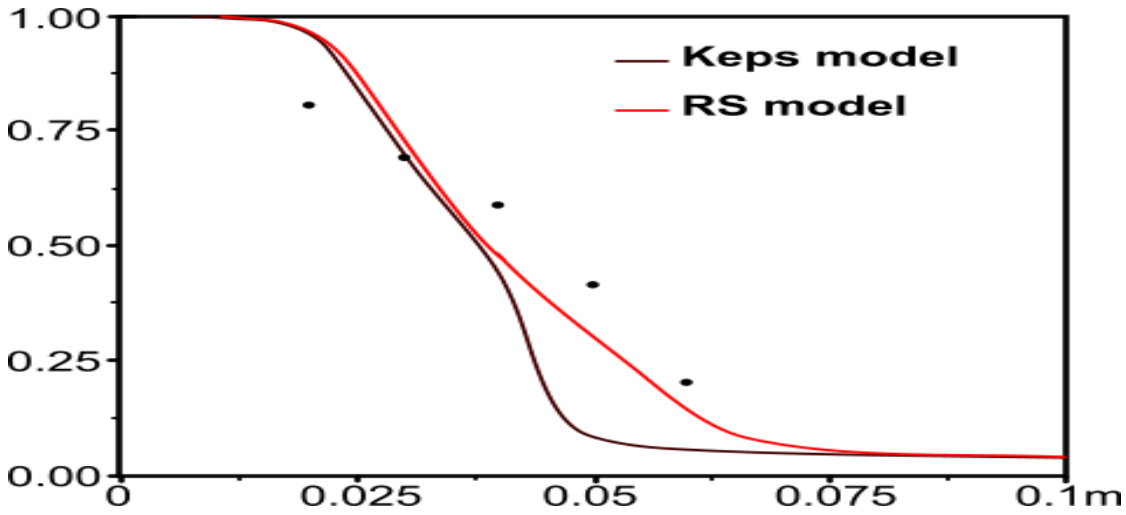

Figure 5: Axial evolution of mean inert scalar on the symmetry axis

The turbulent eddy viscosity fields simulated with k-ε model and RS model are shown in Figure 6. There is a great difference between the two fields especially for a decreasing zone and the stagnation region also. Turbulent viscosity values predicted by k-ε model are much greater than those predicted by RS model, which can explain the low rate of penetration of the methane jet when predicted by k-ε model, and therefore the discrepancies between simulations and measurements shown in figure 4 and 5.

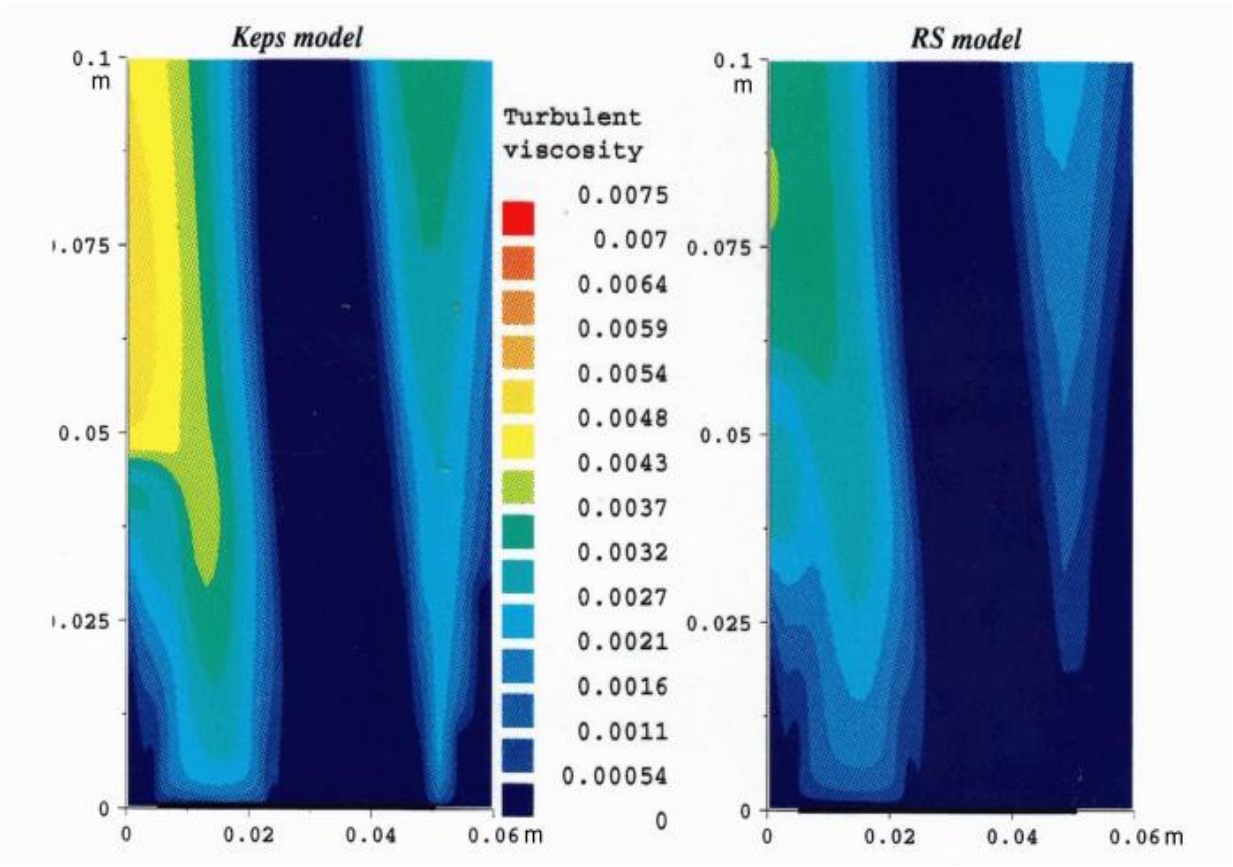

Figure 6: Turbulent eddy viscosity fields predicted by k-ε model (on the left) and RS model (on the right)

The radial evolution of Schmidt number at 50 mm from the burner nozzle is shown in Figure 7**.** It is computed as: $Sc_\theta = \frac{\nu_t}{\widetilde{v''\theta''}} \frac{\partial \tilde{\theta}}{\partial r}$ where $\widetilde{v''\theta''}$ is the radial component of turbulent scalar flux, and r is the radial coordinate.

The Schmidt number is far from constant, especially at the two edges of the recirculation zone where it reaches its maximum value, which is about three times the nearly constant value observed at the center of recirculation zone.

El Amraoui and Garreton [26] have simulated three different round jets, namely the air jet, the CO_2 jet and the Helium jet. They concluded that the Schmidt number is approximately uniform and only slightly depend on the density variation and equal to 0.6±0.1. Sarh [38] shows in a rectangular jet flow that in the slightly heated case the values of the turbulent Prandtl number are more homogeneous and they are between 0.5 and 0.7. In the strongly heated case, these values are generally larger than those from the preceding case and on the other hand, they are more scattered.

These trends were found experimentally by Bahraoui and Fulachier [39] in an air axisymmetric jet.

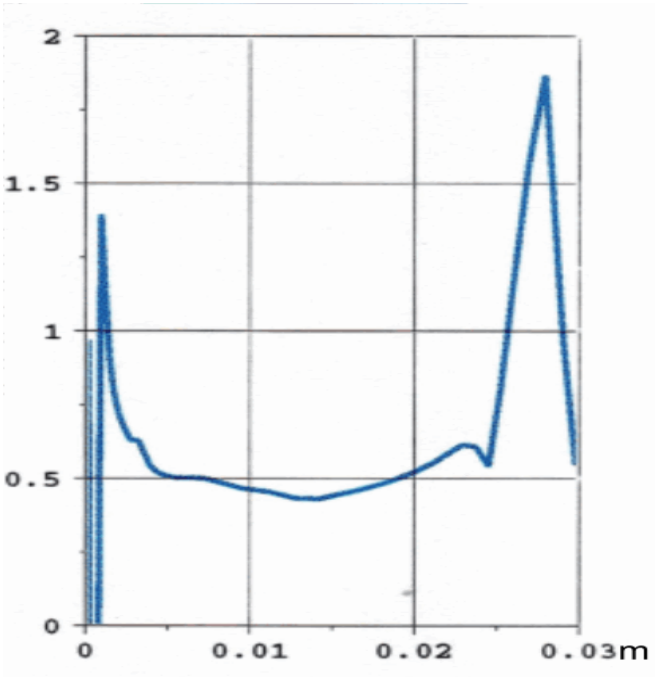

Figure 7: Radial evolution of turbulent Schmidt number at 50 mm

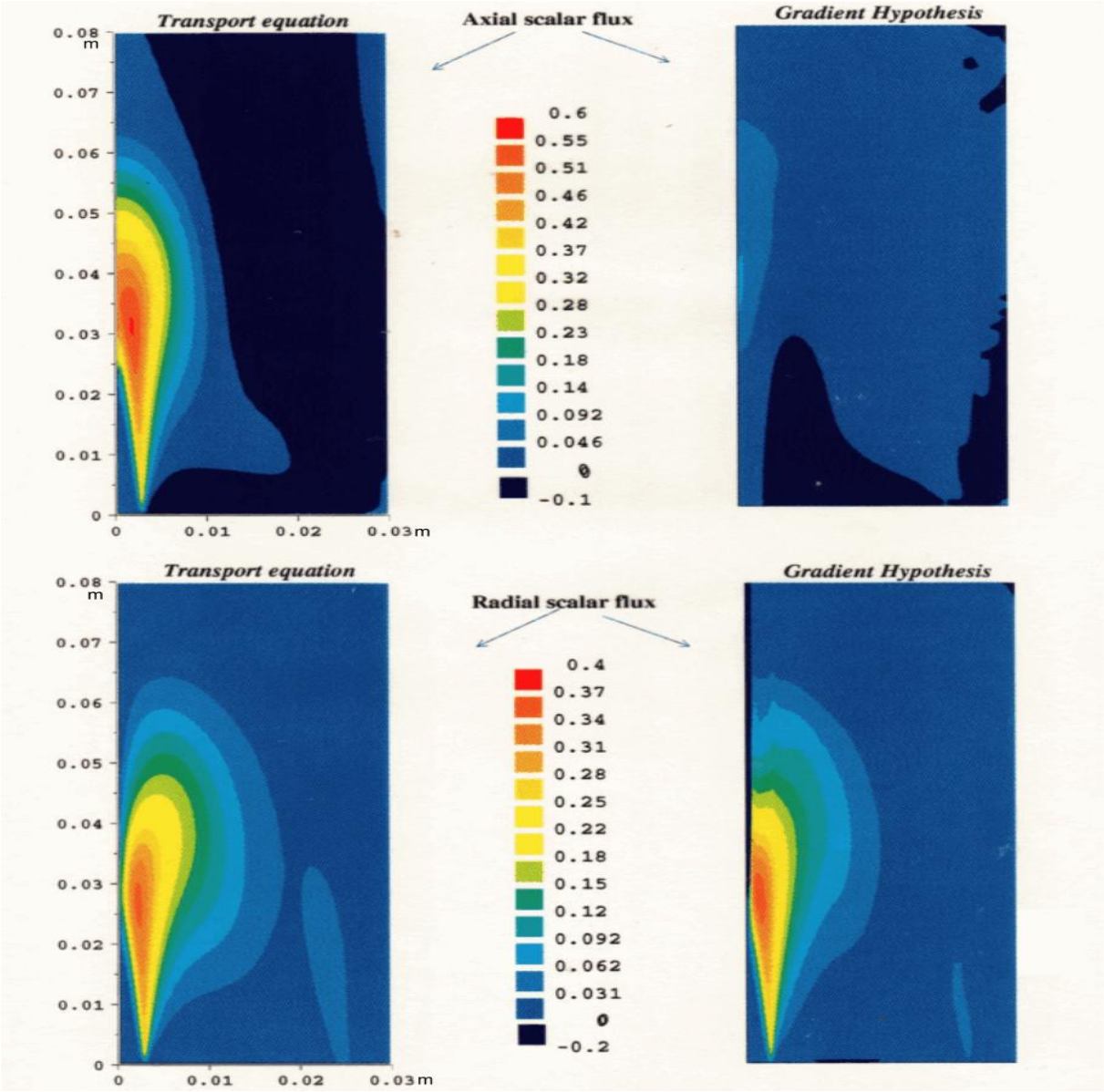

Figure 8: Axial and radial turbulent scalar flux components fields computed with RS model. Comparison between Transport equation and G.T. Hypothesis

Turbulent scalar flux components are shown in Figure 8. Computations have been done using RS model only. Comparisons are made for each scalar flux component between calculation obtained from transport equation and those obtained from gradient transport hypothesis, with Schmidt number equal to 2/3. For the radial scalar flux, calculations are not very different. However an important difference is noted concerning the axial scalar flux. In fact the values obtained from the gradient transport hypothesis are very low compared to those calculated by the transport equation. These results allow us to conclude that if the gradient hypothesis is accepted in the radial direction, it still remains far from reality in the axial direction. A similar result is established in the study of Correa et al. [40] who found that the radial scalar flux component computed from the velocity-scalar joint pdf is approximately the same as that predicted by the gradient transport hypothesis when a Schmidt number is about 0.4.

In the same manner we have computed the axial and radial components of Reynolds stress tensor. Computations were done by RS model. Comparisons are made for each Reynolds stress component between calculations obtained from transport equation and those obtained from gradient transport hypothesis. In this case differences exist between computations for both the axial component but also the radial component (Figure 9). However, they are more pronounced for the axial flux. Moreover the anisotropy of Reynolds stress components is rather well predicted by transport equation.

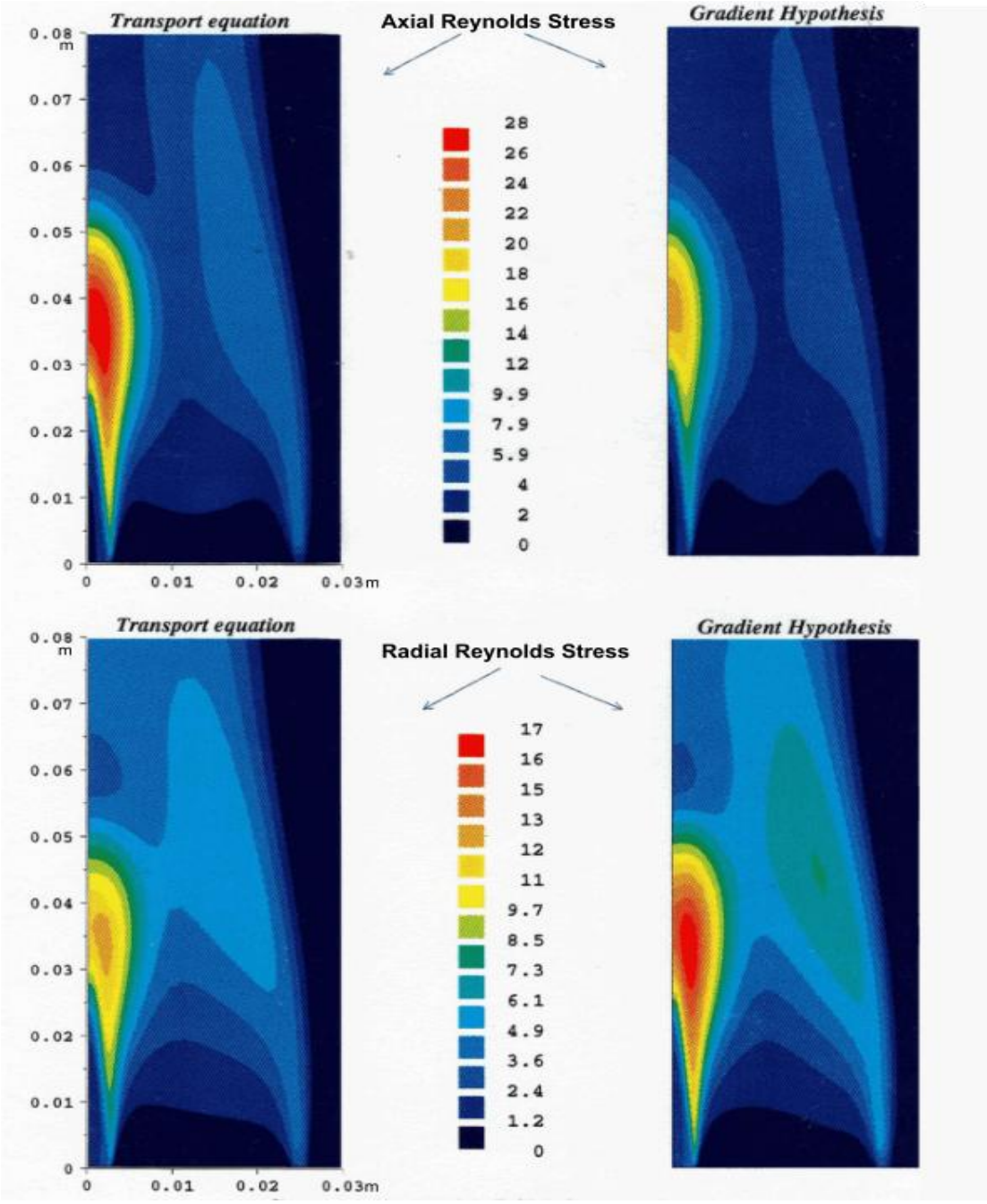

Figure 9: Axial and radial Reynolds stress components fields computed with RS model. Comparison between Transport equation and G.T. Hypothesis

Conclusion

In this study we have examined more closely the validity of the gradient transport hypothesis for the dynamic and scalar fields in the case of a non-trivial turbulent flow exhibiting a complex aerodynamics, such as bluff body one for which a recirculation zone is developed behind the obstacle, and the jet of methane is blocked at the center by the annular air flow. This means that a stagnation point is located on the symmetry axis. The first order turbulence model used is the k-ε. In the second order turbulence model, namely RS model, Reynolds stress and turbulent scalar flux of an inert scalar are transported by their transport equations. Comparison of computations and measurements has showed better prediction of the jet penetration rate by the RS model. This can be explained by the very high values of the turbulent viscosity calculated by the k-ε model, compared to those related to the RS model. In addition, the radial evolution of the turbulent Schmidt number has showed that

it is constant and equal to 0.5, except at the two edges of the recirculation zone where this value is about three times the previous one.
RS model simulations enable us to conclude also that if the gradient transport hypothesis is acceptable in the radial direction, it is not the case for the axial one. Moreover the anisotropy of Reynolds stress components is rather well predicted when second order turbulence model is used.

References

1. Vandromme D., *Thèse d'Etat, Université de Lille* (1983).
2. Prandtl L., Z. Angew. *Math.Mech*. 5 (1925) 136.
3. Launder B.E., Sandham N., *ISBN* -13 978-0-511-06939, (2002) *Cambridge Univ. press*.
4. Launder B.E., Spalding D.B., *Comp. Meth. In Applied Mech.And Engin*.3 (1974) 269.
5. Menter F., *AIAA J.* 32 (1994) 1598.
6. Wilcox D.C., *ISBN* 0-9636051-0-0 (1993) *DCW Industries, California*.
7. Mirzabeygi P., Zhang C., *Int. J. of Heat and Mass transf*., 89 (2015) 229.
8. Dhiri A., Gueraoui K., Taibi M., Lahlou A., *J. Mater. Environ. Sci.* 7 (9) (2016) 3399.
9. Yu H., Thé J. *Atmosph. Environ.* 145 (2016) 225.
10. Lateb M., Masson C., Staphopoulos T., Bédard C., *J. Wind Eng. And Ind. Aerod*. 115 (2013) 9.
11. Medjahed B., Bouzit M., *J. Mater. Environ. Sci*. 7 (12) (2016) 4767.
12. Rahmani K., Al-Kassir A., Benalia M., Djedid M., Ad C., Elmsellem H., Steli H., Kadmi Y., *J. Mater. Environ. Sci*. 8 (2) (2017) 573.
13. Dutta P., Saha S.K., Nandi N., Pal N., *Engin. Sci. and Techn.An Inter. J*. 19 (2016) 904.
14. Bellil A, Benhabib K., Coorevits P., Marie C., Hazi M, Ould-Dris A., *J. Mater. Environ. Sci*. 6 (5) (2015) 1426.
15. Hanjalic K., Launder B.E., *J. Fluid Mech*. 51 (1972) 301.
16. Hanjalic K., Launder B.E., *J. Fluid Mech*. 52 (1972) 609.
17. Daly B.J., Harlow F.H., *Phys. Fluids*, 13 (1970) 2634.
18. Shir C.C., *J. Atmos. Sci*., 30 (1973) 1327.
19. Chou P. Y., *Quart. App. Math.* 3 (1945) 38.
20. Rotta J.C., *Zeitschriftphy sic* 129 (1951) 547.
21. Naot D., Shavit A., Wolfshtein M., *Isr J. Tech*., 8 (1970) 259.
22. Launder B.E., Reece G.J., Rodi W., *J. Fluid Mech*. 68 (1975) 537.
23. Pope S.B., *Cambridge University Press* (2000).
24. Dibble R.W., Kollmann W., Farschi M., Schefer R.W., *Twenty first Symposium (Intern.) on combustion* (1986) 1329.
25. Janicka J., *Twenty first Symposium (Intern.) on combustion* (1986) 1409.
26. El amraoui R., Garreton D., *rep. EDF-DER, HE*. 44./95/014/A (1995).
27. Davidov B.I., *Dolk. Akad.Nauk., SSSR* 136 (1961) 47.
28. Harlow F.H., Nakayama P.I., *Los Alamos Sci. Lab., Univ. of California, rep.* LA-4086 (1968).
29. Gonzalez M., Borghi R., *Seventh Symposium on turbulent shear Flow, Stantford University*, (1989) pp. 23.4.1.
30. Obounou M., Gonzalez M., Borghi R., *Twenty fifth Symposium (Intern.) on combustion* (1994) 1107.
31. Macinnes J. M., *Seventh Symposium on turbulent shear Flow, Stantford University*, (1989) pp.29.3.1.
32. Tailland A., Mathieu J., *Journal de Mécanique*, 6 (1967) 103.
33. Starner S.H., Bilger W., *Eighteenth Symposium (Intern.) on combustion* (1981) 921.
34. Kolmogorov A.N., *Izv. Akad.Nauk.SSSR SeriaFizichiskaVI* (1942) 56.
35. Bilger R.W., *Topics in Applied Physics*, 44 (1980) 65.
36. Schefer R.W., Namazian M., Kelly J., *AIAA Journal*, 32 (1994) 1844.
37. El Amraoui R., Mouqallid M., El Mghari H., Affad E., Obounou M., Garreton D., *J. Mater. Environ. Sc.* 7 (12) (2016) 4361.
38. Sarh B., *Thèse d'Etat, Université Pierre et Marie Currie Paris VI* (1990).
39. Bahraoui E.M., Fulachier L., *Journées d'étude, NOT IMST* 86-10, (1985), *Marseille France*.
40. Correa S.M., Gulati A., Pope S.B., *Twenty fifth Symposium (Intern.) on combustion* (1994) 1167.